Systematic Analysis of Cinnamyl Alcohol Dehydrogenase Family in Cassava and Validation of MeCAD13 and MeCAD28 in Lignin Synthesis and Postharvest Physiological Deterioration

Feifei An , Ting Chen , Wenli Zhu , Xinhui Xiao , Jingjing Xue , Xiuqin Luo , Zhuowen Wei , Kaimian Li , Songbi Chen * , Jie Cai *

Posted Date: 1 October 2024

doi: 10.20944/preprints202409.2434.v1

Keywords: Cassava; cinnamyl alcohol dehydrogenase; gene family; lignin; postharvest physiological deterioration

 doi:10.20944/preprints202409.2434.v1

Article

Systematic Analysis of Cinnamyl Alcohol Dehydrogenase Family in Cassava and Validation of *MeCAD13* and *MeCAD28* in Lignin Synthesis and Postharvest Physiological Deterioration

Feifei An [1,2,†], Ting Chen [3,†], Wenli Zhu [1,†], Xinhui Xiao [1], Jingjing Xue [1,2], Xiuqin Luo [1,2], Zhuowen Wei [1], Kaimian Li [1,2], Songbi Chen [1,2,*,†] and Jie Cai [1,2,*]

[1] Tropical Crops Genetic Resources Institute, Chinese Academy of Tropical Agricultural Sciences/Key Laboratory of Ministry of Agriculture for Germplasm Resources Conservation and Utilization of Cassava, Haikou 571101, China
[2] National Key Laboratory for Tropical Crop Breeding, Sanya 572025, China
[3] Postgraduate Department, Hainan normal university, Haikou 571158, China
* Correspondence: songbichen@catas.cn; caijie@catas.cn
† These authors contributed equally to this work.

Abstract: Cassava (*Manihot esculenta* Crantz) is used as biomass energy materials and an effective supplement for food and feed. Cinnamyl alcohol dehydrogenase (CAD) catalyzes the final step of lignin biosynthesis and is responsible for various stresses. However, systematic investigation of *CAD* gene family in cassava has been poorly understood. In this study, we performed a genome-wide survey and identified 36 *MeCAD*s genes that were unevenly harbored in 12 chromosomes. Through phylogenetic analyses along with *Arabidopsis* counterparts, these MeCADs were divided into four groups, each gene contains a similar structure and conserved motifs. Interestingly, transcriptome data analyses unveiled 32 *MeCAD* genes during the postharvest physiological deterioration (PPD) process of cassava tuberous roots, whereas 27 *MeCAD* genes significantly changed. Meanwhile, the relative quantitative analysis of 6 *MeCAD* genes demonstrated that they were sensitive to PPD, suggesting they may involve in PPD regulation. Silencing *MeCAD13* and *MeCAD28* further showed that lignin content significantly decreased in the leaves. The wound-stress tolerance of transgenic yeast cells was enhanced after transformation with *MeCAD13* and *MeCAD28*. In conclusion, *MeCAD13* and *MeCAD28* may play positive roles in lignin biosynthesis and PPD response, respectively. These results provided a systematic functional analysis of *MeCADs* in cassava and paved a new way to genetically modify of lignin biosynthesis and PPD tolerance.

Keywords: Cassava; cinnamyl alcohol dehydrogenase; gene family; lignin; postharvest physiological deterioration

1. Introduction

Cassava (*Manihot esculenta* Crantz) is a vital crop that plays a significant role in global food security because of its carbohydrates and essential nutrients, particularly in regions where it serves as a staple food source for millions of people [1]. Its global production was 330 million tons in 2022 (FAOSTAT) [2]. However, cassava faces challenges during postharvest handling and storage, with postharvest physiological deterioration (PPD) being a major concern that affects the quality and market value of tuberous roots [3]. Mechanical damages caused by collision, vibration, and extrusion during harvesting and storage are the main causes of PPD [4]. Then, a series of biochemical and physiological changes occurs, leading to typical phenomenon such as rapidly tissue deterioration, discoloration, and loss of firmness. Ultimately, nutritional quality decreases and susceptibility to microbial decay increases [5]. The main research on PPD primarily focuses on reactive oxygen species (ROS) elimination, programmed cell death [6–10]. Furthermore, wound healing can maintain the

 doi:10.20944/preprints202409.2434.v1

shelf life of tuberous roots by preventing water evaporation, nutrient outflow and pathogen infection [11–13]. The wound healing of cassava tuberous root is reportedly too late or inadequate to prevent the PPD response [14]. Therefore, deepening the research on cassava wound healing has become very necessary.

The phenylpropanoid metabolism pathway regulates wound healing by synthesizing phenolic compounds, lignin, and suberin [15]. For instance, activating phenylpropane metabolic pathway can promote wound healing in potato tubers [16]. Lignin is a phenolic heteropolymer in secondary cell walls, which plays a major role in mechanical support and defense against biotic and abiotic stresses, as well as affects the quality of fruits [17–21]. The biosynthesis of lignin involves many enzymes and corresponding genes, in which cinnamyl alcohol dehydrogenase (CAD) catalyzes the final step in monolignols biosynthesis [22]. Decreased lignin content has been reported in CAD down-regulation plants [23,24]. CADs are also involved in various stresses, such as drought and salinity stresses [25,26]. Until now, CAD gene families have been identified in many plants, including Arabidopsis [23], rice [27], poplar [28], mulberry [29], and pear [30]. However, the genome organization, gene structure, and expression profiling in PPD of *MeCAD* gene family in cassava is poorly understood.

In the present study, we identified the members of the *MeCAD* gene family in cassava, and then analyzed their phylogenetic relationships, gene structures, conserved motifs, synteny, and expression patterns with the PPD transcriptomic data. Additionally, the function of 2 *MeCADs* in lignin biosynthesis was verified by subjecting transgenic cassava to virus-induced gene silencing (VIGS). Our finding can provide a foundation for the in-depth functional analysis of *MeCAD* genes, as well as understanding the mechanisms underlying PPD regulation. Accordingly, effective postharvest management strategies can be developed to prolong the shelf life of tuberous roots and minimizing PPD losses.

2. Results

2.1. Identification and Phylogenetic Analysis of CAD in M. esculenta

A total of 36 CAD proteins were characterized from *M. esculenta* and denoted as MeCAD1 to MeCAD36, respectively. All MeCADs contained the CAD domain based on SMART tests and Pfam analysis **(Figure S1)**. The MeCAD proteins' lengths ranged from 353 (MeCAD28) to 435 (MeCAD17) amino acids, MW from 38.41 to 47.36 kDa, and p*I* from 5.50 to 8.22. Among the 36 MeCAD proteins, one was predicted to be peroxisomes protein (MeCAD10), five were located in the chloroplast (MeCAD17, 20, 22, 23 and 32), one was cytoskeleton protein (MeCAD18). The rest were localized in the cytoplasm. Detailed information including CAD name, gene accession, chromosome locus, protein length, MW, p*I* of all MeCAD proteins were shown in **Table S1**.

The CAD domain sequences of 36 MeCAD proteins, 12 OsCAD proteins and 9 AtCAD proteins were used to construct a phylogenetic tree through NJ method. Results indicated that the 36 MeCADs were classified into four groups **(Figure 1)**. Group V contained the highest CAD members with 16 MeCADs, followed by group I with 14 MeCADs. Group IV and Group III had the least CAD members with only 3 MeCAD. However, Group II only including 8 OsCAD proteins. MeCAD13, MeCAD15 and MeCAD28 were clustered in group IV, including AtCAD4, AtCAD5 and OsCAD2, which were primary genes involved in lignin biosynthesis in *Arabidopsis* [31]. This finding suggested that CAD members in group IV of cassava con be the important genes involved in lignin biosynthesis in cassava.

 doi:10.20944/preprints202409.2434.v1

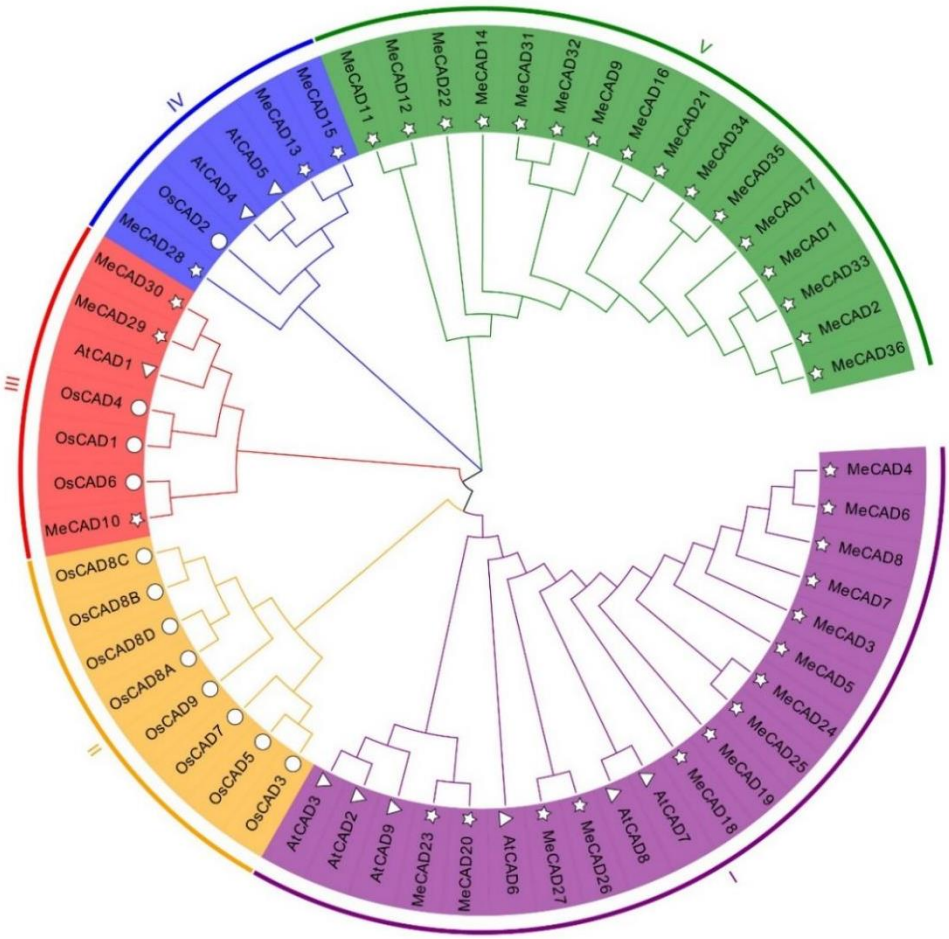

Figure 1. Multiple sequence alignment of CAD domain sequences of *M. esculenta* and *A. thaliana* was performed using Clustal W. ☆ indicate CADs in *M. esculenta*, △ indicate CADs in *A. thaliana.* ○ indicate CADs in *O. sativa.*

2.2. Chromosomal Locations, Duplications, and Synteny Analysis of the MeCAD Genes

A total of 36 *MeCAD* were mapped on 12 chromosomes, and the distribution on each chromosome was uneven (**Figure 2**). For instance, chromosome 02 and 13 contained eight *MeCAD* genes, individually. however, chromosome 01, 05, 06, 07, 08, 10, 14 and 16 contained only one *CAD* genes on each chromosome. Interestingly, many *MeCAD* genes such as chromosome 02, 13 and 18 were clustered in a short distance. Six pairs (*MeCAD2*/*MeCAD33*, *MeCAD13*/*MeCAD15*, *MeCAD15*/*MeCAD28*, *MeCAD16*/*MeCAD21*, *MeCAD18*/*MeCAD25* and *MeCAD20*/*MeCAD23*) of segmental duplications were identified in total **(Figure 3 and Table S2)**. To detect the synteny of *CAD* genes, a collinearity analysis between *M. esculenta*, *A. thaliana* and *O. sativa* using MCScanX was performed. We found 7 paired collinearity relationships between 5 *MeCAD* and 4 *AtCAD* genes, as well as 1 paired collinearity relationships between 1 *MeCAD* and 1 *OsCAD* **(Figure S2 and Table S3)**.

Preprints.org (www.preprints.org) | NOT PEER-REVIEWED | Posted: 1 October 2024 doi:10.20944/preprints202409.2434.v1

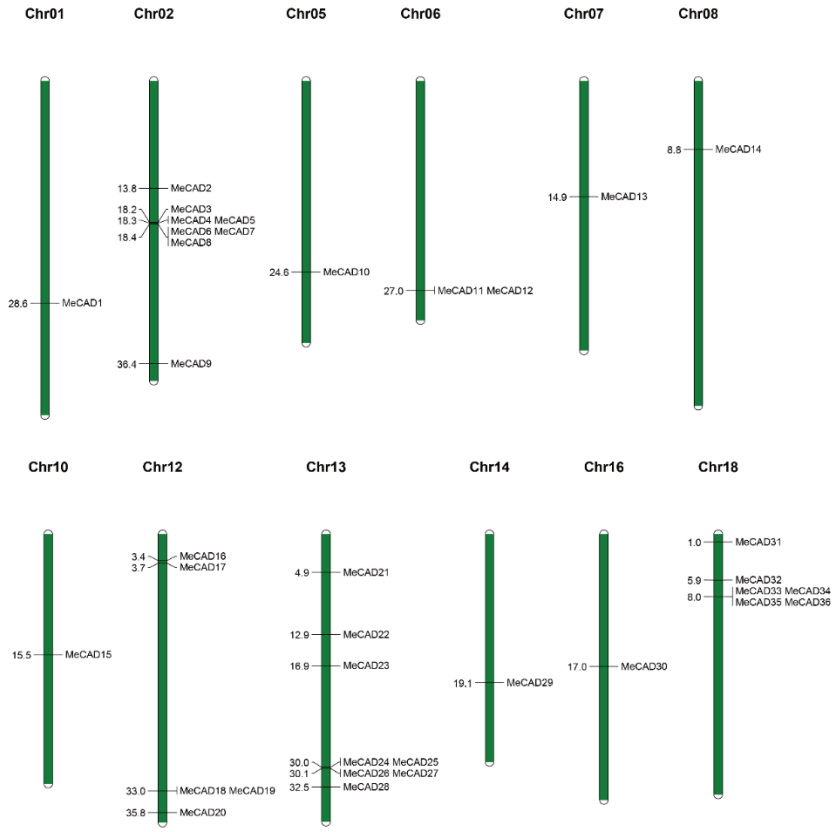

Figure 2. Chromosomal locations of *MeCAD* genes. Green bars denote the *Manihot esculenta* chromosome. Scale bar on the left indicates the chromosome lengths (Mb).

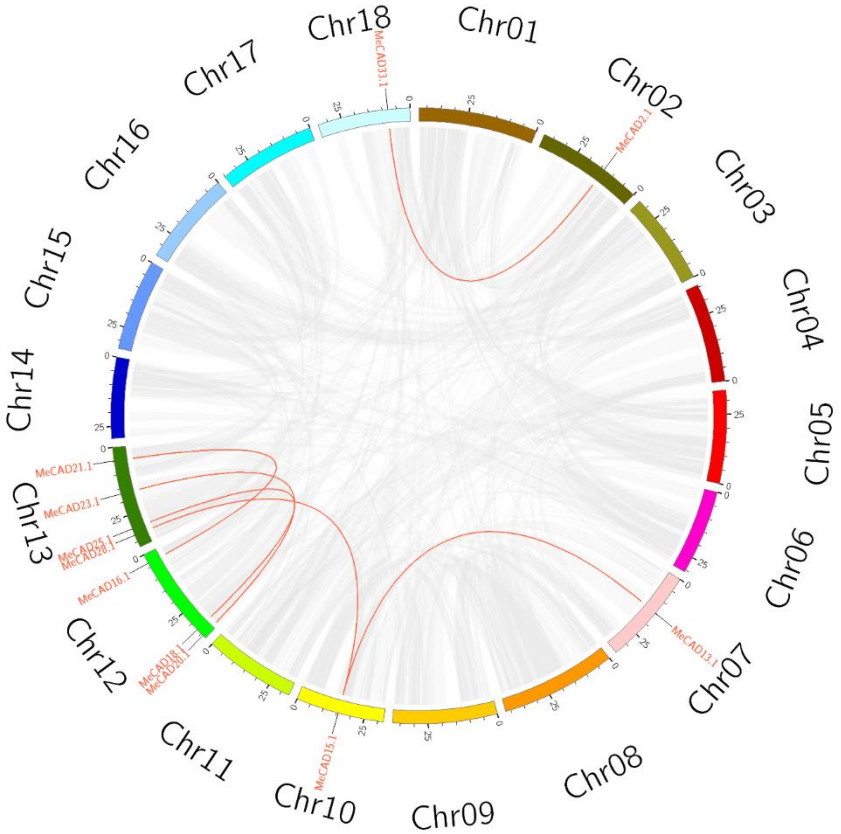

 doi:10.20944/preprints202409.2434.v1

Figure 3. Circos diagram of the *MeCAD* duplication pairs in *M. esculenta. MeCAD* duplication pairs are linked with red lines.

2.3. MeCAD Structure, Conserved Motifs and Cis-Acting Regulatory Element

The exon/intron organization and conserved motifs of all *MeCAD* genes were analyzed **(Figure 4)**. The exon number ranged from 5 to 10, and 10 *MeCAD* genes contained 10 exons, the highest number of all genes. They included *MeCAD1, MeCAD2, MeCAD9, MeCAD17, MeCAD31, MeCAD32, MeCAD33, MeCAD34, MeCAD35, MeCAD36.* Meanwhile, *MeCAD14* contained 7 exons, *MeCAD22* contained 8 exons, *MeCAD16 and MeCAD21* contained 9 exons, *MeCAD10, MeCAD11, MeCAD12, MeCAD29,* and *MeCAD30* contained 6 exons, and the other 17 *MeCAD* genes contained 5 exons. Additionally, *MeCAD* genes in the same group had similar gene structure. Notably, members with high similarity in the same group shared a common motif composition. For instance, MeCAD13, MeCAD15 and MeCAD28 were found to contain 7 motifs. Thus, there three genes may have similar functions. MeCAD proteins contain 4-7 conserved motifs. However, only MeCAD12 contained 4 motif and 2 MeCAD proteins (MeCAD11, MeCAD22) contained five motifs. A total of 15 MeCAD proteins and 18 MeCAD proteins contain 6 motifs and 7 motifs, individually.

Figure 4. Putative conserved motifs and gene structures of *MeCAD* genes. MEME analysis revealed the conserved motifs of MeCAD proteins. The colored boxes on the right denote 10 motifs. The yellow boxes, black lines, and green boxes represent exon, intron, and untranslated region (UTR), respectively.

The *cis*-acting regulatory elements of each *MeCAD* promoter were characterized using PlantCARE and PLACE database. The most 10 *cis*-acting regulatory elements were founded in *36 MeCADs* **(Figure S3)**. The common regulatory elements such as CAAT-box and TATA-box were presented in all 36 *MeCAD* genes. We also identified *cis*-acting regulatory elements related to hormone responses, namely, MYB, ABRE and ARE, which were involved in abscisic acid (ABA) responsiveness. ERE, MeJA responsive elements. Interestingly, the promoter of 26 *MeCAD* genes contained elements related to wounding (WUN-motif), as well as other elements related to biotic and abiotic stress, such as drought (MBS), pathogen defense (W-box). In summary, *MeCAD* genes can be regulated by diverse hormone and different environment.

 doi:10.20944/preprints202409.2434.v1

2.4. Expression Profile of MeCADs and Lignin Changes in Response to PPD

The expression levels of *MeCADs* in tuberous roots during PPD were analyzed by RNA-seq data. A total of 32 (88.89%) *MeCAD* genes exhibited differences in their expression levels in response to PPD **(Figure 5A)**. Additionally, 27 *MeCADs* showed significant differences in compared with the control. Among them, 6 up-regulated genes (*MeCAD9*, *MeCAD11*, *MeCAD13*, *MeCAD16*, *MeCAD26*, *MeCAD28*) were verified by qRT-PCR in PPD samples. Thus, the expression of 6 *MeCAD* genes remarkably increased as PPD progressed **(Figure 5B)**. However, the expression levels of *MeCAD9*, *MeCAD28* at 5 d were less than those at 3 d, but still higher than those at 0 d. These results showed no significant difference with RNA-seq, where they were all up-regulated compared with those at 0 d.

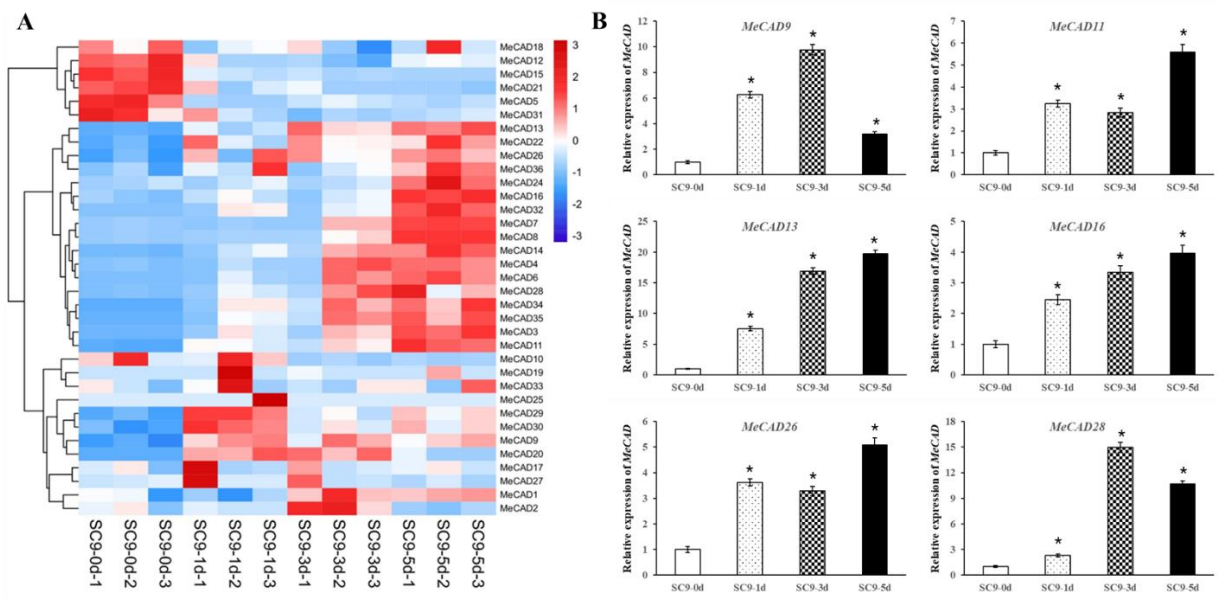

Figure 5. Expression profiles of *MeCAD* genes in tuberous roots during PPD process and qRT-PCR results for 6 *MeCADs*. (A) The heat map was generated by Mev software. The bar on the right of the heat map indicates relative expression values. Values 3, 0, -3 represent high, intermediated, and low expression, respectively. (B) qRT-PCR was used to analyze the expression profiles of 6 up-regulated *MeCAD* genes according to RNA-seq. The relative expression levels are normalized to *MeActin*. The data represent the mean of three biological replicates. The x-axis represents four materials from different PPD stage. The y-axis represents the relative expression levels of *MeCADs*. All data are the Means±SE of three independent experiments. Error bars indicate the standard deviation.

Lignin biosynthesis was associated with PPD process, so we also detected the lignin content in tuberous roots during PPD. Results showed that lignin content significantly increased with PPD degree. The lignin content in tuberous roots was 67.45 μg/mg after harvest, whereas on the 1st, 3rd and 5th after harvest, the values were 69.22, 70.16 and 72.22 μg/mg, respectively **(Table 1)**.

Table 1. Lignin content of tuberous roots in four PPD samples and leaves infected with CsCMV-CAD13 and CsCMV-CAD28.

Content (μg/mg)	Tuberous roots				Leaves		
	SC9-0d	SC9-1d	SC9-3d	SC9-5d	CsCMV-NC	CsCMV-*CAD13*	CsCMV-*CAD28*
Lignin	67.45 ± 0.43 d	69.22 ± 0.20 c	70.16 ± 0.44 b	72.22 ± 0.48 a	25.39 ± 0.47 a	10.14 ± 0.20 c	14.89 ± 0.27 b

One-way ANOVA (Tukey) was conducted for difference significance test, and different letters in the same row represented extremely significant difference (P<0.05).

 doi:10.20944/preprints202409.2434.v1

2.5. MeCAD13 and MeCAD28 Were Necessary for Lignin Biosynthesis and Wound Response

Tissue-specific expression of *MeCAD13* and *MeCAD28* revealed that *MeCAD13* was primarily expressed in tuberous roots and *MeCAD28* was primarily expressed in fibrous roots **(Figure S4)**. We also investigated the subcellular localization of MeCAD13 and MeCAD28 proteins *in planta.* Consistent with a previous study, GFP-fused MeCAD13 protein was localized in cytoplasm, and GFP-fused MeCAD28 protein was localized in cytoplasm even in tobacco leaves **(Figure 6A)**, indicating their similar localization with prediction in **Table S1.** To study the *in vivo* roles of *MeCADs* in cassava lignin biosynthesis, two gene-silenced cassava lines were constructed (*pCsCMV-CAD13* where *MeCAD13* was silenced, and *pCsCMV-CAD28* where *MeCAD28* was silenced). The phenotypes between *MeCADs*-silenced lines and control plants are shown in **Figure 6B**. When the transcript levels of *MeCAD13* and *MeCAD28* were evaluated in *MeCAD*-silenced lines, the transcripts level of targeted *MeCADs* were drastically reduced compared with pCsCMV-NC (**Figure 6C**). We compared the lignin content of *MeCADs*-silenced lines in leaves with that of control plants, and found that lignin content significantly decreased in the leaves with *MeCAD13*- and *MeCAD28*-silenced lines **(Table 1)**. In summary, the lignin content in pCsCMV-NC (control) leaves was 25.39 μg/mg, whereas the lignin content in the leaves of *MeCAD28*-silenced lines was 14.89 μg/mg, a decrease of 41.35% compared with the control. However, the lignin content in the leaves of *MeCAD13*-silenced lines decreased more significantly than in *MeCAD28*-silenced lines, reaching 60.06%. Therefore, *MeCAD13* and *MeCAD28* may be candidate genes involved in lignin biosynthesis, and the function of *MeCAD13* in lignin synthesis may be superior to that of *MeCAD28.*

To understand the response of *MeCAD13* and *MeCAD28* to wound stress, the genes were transferred into yeast cells, and the growth of yeast cells was observed by simulating mechanical wound stress with upon systemin addition. As shown in **Figure S5**, the growth of pDR196-*MeCAD13* and pDR196-*MeCAD28* transgenic yeast strains was better than that of pDR196 empty vector after mechanical wound treatment. This indicated that the expression of *MeCAD13* and *MeCAD28* in yeast improved the tolerance of transgenic yeast cells to mechanical wound and enhanced their growth status.

 doi:10.20944/preprints202409.2434.v1

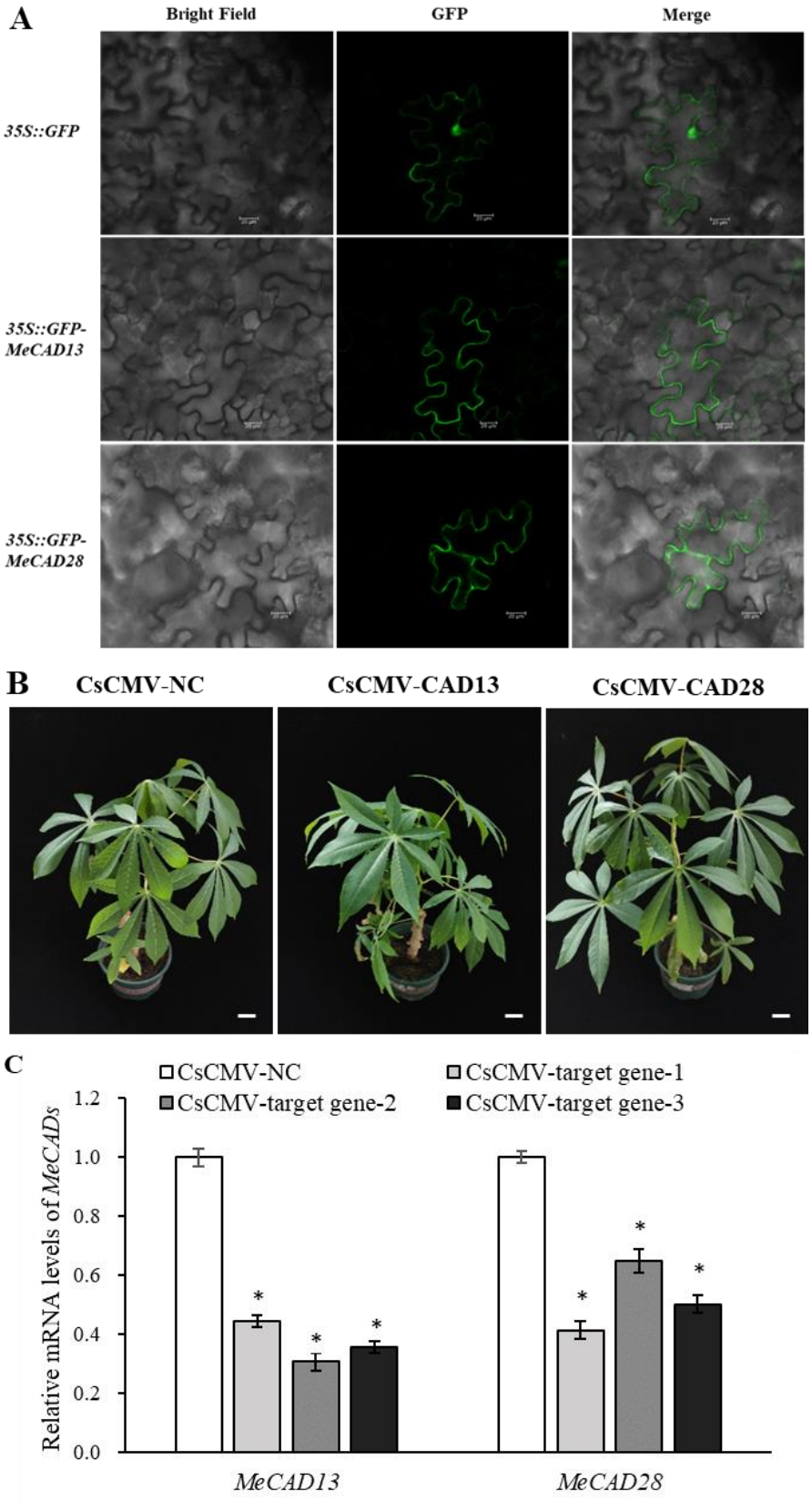

Figure 6. Subcellular localization and Silencing of *MeCAD13, MeCAD28* using the pCsCMV-*CAD13* and pCsCMV-*CAD28*. (A) Subcellular localization of MeCAD13 and MeCAD28 in tobacco leaves. Bars = 20 μm. (B) Silencing phenotypes in *M. esculenta* using the pCsCMV-*CAD13* and pCsCMV-*CAD28* at 25 dpi. CsCMV-NC means infected with non-target control pCsCMV-NC. Bars = 1 cm. (C) qRT-PCR analyses of *MeCAD13* and *MeCAD28* mRNA expression in *M. esculenta* infected with

 doi:10.20944/preprints202409.2434.v1

pCsCMV-*CAD13* and pCsCMV-*CAD28*. Three independent experiments were performed and each included three plants per treatment group. Error bars indicate the standard deviation.

3. Discussion

CAD is a major rate-limiting enzyme in lignin biosynthesis. It is related to stress responses, and is also closely associated with vegetative tissue and aging [32,33]. The CAD gene family has been identified and functionally analyzed genome-wide in many plant species, such as Arabidopsis [23], rice [27], wheat [34], sweet potato [17], sorghum [35], tea [36]. The present study aimed to identify and analyze CAD genes in cassava, as well as explore the candidate *MeCADs* genes for regulating lignin synthesis and PPD. A total of 36 *MeCAD* gene members were identified in cassava genome, and the number was higher than those in Arabidopsis and rice. The reason for the increase in *MeCAD* numbers may be the genome of "AM560" or the gene duplication events.

We subsequently analyzed and predicted gene functions through phylogenetic-tree analysis. Results revealed that 36 *MeCADs* can be classified into four subfamilies **(Figure 1)**, *MeCAD13/15/28* were clustered in cluster IV with *AtCAD4/5* and *OsCAD2*. *AtCAD4* and *AtCAD5* in cluster IV played an important role in the biosynthesis of lignin in *Arabidopsis thaliana* [31], also *OsCAD2* in *Oryza sativa* [37]. We speculated that the CADs of cluster IV in cassava may have a function similar to lignin synthesis. In our study, the lignin content significantly decreased in *MeCAD13* silenced and *MeCAD28* silenced leaves, especially in *MeCAD13* silenced lines **(Table 1)**. Therefore, *MeCAD13* and *MeCAD28* were the key genes involved in lignin synthesis in cassava. Furthermore, the homologous *CAD* genes may participate in lignin biosynthesis in one type of tissue during different developmental stage or different tissues [38]. For example, *AtCAD4* was strongly expressed in flowers and roots, and *AtCAD5* was expressed in lignified roots and strongly expressed in pathogen-infected tissues [39]. *MeCAD13* was strongly expressed in tuberous roots, *and MeCAD28* was strongly expressed in fibrous roots **(Figure S4)**. *MeCAD10/29/30* were clustered in cluster III with *OsCAD1/4/6*, consistent with a previous finding that *OsCAD6* is not directly involved in lignin biosynthesis, but may be participated in lignans [27]. We speculated that *MeCAD10/29/30* may be correlated with lignans synthesis. No *MeCAD* and *AtCAD* family members were in cluster II with 8 *OsCADs*, and cluster V included only 16 *MeCADs*, which was probably due to the methods and protein sequences. Notably, the function of *MeCADs* in these cluster requires further elucidation.

Gene duplication plays an essential role in species evolution and gene family evolution [40]. In this study, we identified six pairs of segmental duplications, while no tandem duplications in cassava **(Figure 3 and Table S2)**. Tandem duplicated genes were relatively less, consistent with the results in tobacco [41]. Thus, segmental duplication was the main duplication model in cassava genome. A large number of hormone response elements (ABA, MeJA) and stress response elements (wound, drought) were founded in *MeCAD* gene promoter **(Figure S3)**. It implied that *MeCAD* genes may be involved in various stress responses and can be induced by many hormones. For example, ABA has been shown to induce CADs gene expression in sweet potato after exposure to abiotic stress [17]. ABA-induced *CmCADs* expression is reportedly related to the upstream MYB response elements [32], whereas 32 *MeCAD* genes contained MYB elements in promoter regions. Nevertheless, this speculation should be demonstrated by further cloning and function analyses of *MeCAD* promoter. The hormone regulation on different *MeCAD* gene members, and the complex hormonal regulation of *MeCAD* genes under different stress conditions also warrant further investigation.

The phenylpropanoid pathway genes including *CADs* are closely related with biotic and abiotic stresses, including lignin deposition in secondary cell walls and defense-related compounds biosynthesis [42–44]. As mentioned above, the overexpression of *MeCAD13* and *MeCAD28* also enhanced the wound resistance of yeast **(Figure S5)**. PPD is a kind of mechanical damage caused by wound, the transcriptional expression and enzyme activity of CAD continuously increased, and a net-like lignin layer formed in wound sites of SC9 tuberous roots [45]. A total of 32 *MeCAD* genes responded to PPD, whereas 27 *MeCAD* genes significantly changed, among which 6 were verified by qRT-PCR **(Figure 5)**. These results were consistent with the changes in CAD enzyme activity in tuberous roots [6]. Lignin accumulation forms a physical barrier to limit pathogens invasion [46],

 doi:10.20944/preprints202409.2434.v1

thereby preventing the rapid postharvest deterioration of cassava roots [45]. Lignin content increased in cassava tuberous roots after PPD initiation, and significantly increased with prolonged storage time **(Table 1)**, which may be due to the up-regulation expression of *MeCAD* genes. Wound healing involves cell wall reinforcement by lignin and other phenolic compounds, in which phenylpropane metabolism plays a vital role [15]. Phenylpropane metabolism was activated after cassava root injury indicated by an increase of phenylalanine ammonia-lyase (PAL) enzymatic activity, coupled with cinnamic acid 4-hydroxylase (C4H), 4-coumarate-CoA ligase (4CL) and CAD [45]. Moreover, MeCAD13 can interacted with MePOD12, delaying PPD occurrence through ROS elimination [6]. All these finding indicate that *MeCADs* are closely related with PPD regulation in cassava tuberous roots, whereas the specific functions of *MeCADs* in PPD remains to be demonstrated.

4. Materials and Methods

4.1. Plant Materials

The tuberous roots of South China 9 (SC9) were harvested after planting for 10 months. They were located in the National Cassava Germplasm Repository, Danzhou, Hainan, China. The tuberous roots then cultivated in a chamber at 26 °C and a 16/8 h photoperiod (day/night). After 1, 3 and 5 days, the tuberous roots were selected as materials, and PPD score was determined according to Rahmawati et al [47]. All samples were collected and frozen in liquid nitrogen immediately and stored at -80 °C for further analysis. For VIGS analysis, nine SC9 plants were inoculated with the recombinant VIGS vector after 25 days post inoculation (dpi). Leaves, petiole, stem, FEC, flowers, buds, fibrous roots, and tuberous roots of SC9 were used for tissue-specific analysis. *Nicotiana benthamiana* was used for subcellular localization.

4.2. Identification of MeCAD Genes in Cassava Genome

The whole genome sequences (v. 8.0) of cassava were downloaded from the phytozome database (https://phytozome-next.jgi.doe.gov/). The Hidden Markov Model (HMM) profile of CAD (PF00107 and PF08240) was retrieved from Pfam (http://pfam.sanger.ac.uk/). The HMMER program was used to search for CAD protein in cassava genome, and then all putative proteins were further filtered by e-Value < 0.001 and confirmed by Pfam and SMART database (http://smart.embl-heidelberg.de/). The molecular weight (MW) and theoretical isoelectric point (p*I*) of these proteins were predicted by ExPASy (https://www.expasy.org/). Finally, we named the proteins according to their locations on the chromosomes. Subcellular localization of MeCADs was predicted by WoLF PSORT (https://wolfpsort.hgc.jp/).

4.3. Chromosomal Mapping, Gene Structure, Conserved Motif, and Cis-Acting Regulatory Element Analysis

Chromosomal mapping of these *MeCAD* genes was constructed by MapChart program (v. 2.32). Gene structures were visualized using GSDS2.0 (http://gsds.gao-lab.org/). Additionally, the online software MEME (http://meme-suite.org/tools/meme) was used to identify the conserved motifs among all *MeCAD* genes. The number of motifs was set to 10. Then, 2000 bp upstream sequences of transcription start site ATG were extracted as the promoter sequence and screened using PlantCare (http://bioinformatics.psb.ugent.be/webtools/plantcare/html/) before finally visualizing with GSDS2.0.

4.4. Phylogenetic Analysis, Gene Duplication, Multiple Alignments, and Synteny Analysis

Clustal W was performed for the multiple sequence-alignment analysis of CAD domain sequences. MEGA 11 was used to constructed the phylogenetic tree with the neighbor-joining (NJ) method. Clustal X (V.2.0) program was used to compare the coding sequences of repeated genes. Circos program was used to illustrate the relationships of duplicated genes. The synteny of *CAD* genes between *Manihot esculenta*, *Arabidopsis thaliana* and *Oryza sativa* was detected by MCScanX.

 doi:10.20944/preprints202409.2434.v1

4.5. RNA-seq Analysis and qRT-PCR Verification

The tuberous roots of SC9 were storage for 0, 1, 3 and 5 days and used for transcriptome analysis, the platform for transcriptome sequencing was Illumina (HiSeq X-Ten), and three biological repeats were implemented for each sample. Heat maps were drawn using Mev software. Total RNA was extracted from 3 g of tuberous roots by using a RNAprep Pure Plant plus Kit (Tiangen, China). One-Step gDNA Removal and cDNA Synthesis SuperMix (TransGen, China) was used for first-strand cDNA synthesis. The qRT-PCR reactions were performed in 10 μL volume in a thermocycler (Thermo Fisher Scientific Inc., Göteborg, Sweden). The qRT-PCR primers were shown in **Table S4**. The reference gene of *MeActin* served as an internal reference. All experiments of each gene were performed in triplicate per sample. The formula $2^{-\triangle\triangle Ct}$ method was used to calculate the relative gene expressions.

4.6. Gene Cloning, Expression and Subcellular Localization of MeCAD13 and MeCAD28

Full-length *MeCAD13* and *MeCAD28* were amplified by PCR using the cDNA of SC9 tuberous roots as a template. They were then inserted into the transient expression vector pNC-Green-SubN to generate *35S::GFP-MeCAD13* and *35S::GFP-MeCAD28* recombinant vector, respectively [48]. **Table S5** lists the primers used for subcellular localization and sequencing. *Agrobacterium tumefaciens* strain GV3101-psoup was co-transformed with the recombinant plasmid, and then transiently expressed in *Nicotiana benthamiana* leaves, as described by An et al. [40]. pNC-Green-SubN served as the positive control. The GFP signal (395-509 nm) were observed with a laser scanning confocal microscope (TCS SP8, Leica) after 3 days.

4.7. Virus-Induced Gene Silencing (VIGS) in Cassava and qRT-PCR Verification

For vector construction, 300 bp *MeCAD13* and *MeCAD28* DNA fragments were cloned into pCsCMV-NC as described by Tuo et al. [49]. The primers were listed in **Table S5**. The recombinant plasmid was co-transformed in *A. tumefaciens* strain GV3101-psoup, and cultured at 28 °C in chamber before resuspending in 10 mM MES, 10 mM $MgCl_2$ and 100 μM acetosyringone. The preparations were injected into the back of cassava leaves by using syringe and grown in greenhouse for 23 days. The expression level of the target gene in *MeCAD13* and *MeCAD28* silenced lines was detected, and the qRT-PCR primers are shown in **Table S4**.

4.8. Quantitative Analysis of Lignin

The Lignin content in tuberous roots and leaves of cassava were measured as described in Foster et al. [50], with minor modification. The main method involved using acetyl bromide to dissolve lignin in the sample, followed by determining the total lignin content through a colorimetric method. A multi-mode microplate reader (Multiskan GO, Thermo Fisher Scientific, USA) was used for the quantitative analysis of lignin content.

4.9. Stress of Yeast W303

The CDS of *MeCAD13 and MeCAD28* was amplified (the specific primers are listed in **Table S5**), and then inserted into the pDR196 vector. The pDR196-*MeCAD13* and pDR196-*MeCAD28* construct were then transformed into *Saccharomyces cerevisiae* W303. After transformation, the yeast cells were streaked on SD-Ura medium and grown overnight in liquid SD-Ura medium. After the adjustment to optical density (OD) $_{600}$=1.0, the cells were centrifuged briefly for 30 s, the supernatant was discarded, 20 nM systemin (wound stress) was added. Serial dilutions (OD_{600} = 0.1, 0.01, 0.001) were plated on the SD-Ura medium. The plates were incubated at 30 °C for 3 days and photographed.

 doi:10.20944/preprints202409.2434.v1

4.10. Statistical Analysis

Excel 2019 and Statistical Product and Service Solution program（version 20, SPSS Inc., Chicago, IL, USA）were used for all statistical analyses. One-way ANOVA (Tukey) was conducted for comparisons of the expression level and lignin content in cassava leaves.

5. Conclusions

A genome-wide analysis of *MeCAD* gene family was conducted with particular focus on their response to cassava PPD and lignin synthesis. A total of 36 *MeCAD* genes were identified and characterized, unevenly harbored in 12 chromosomes. Four subfamilies were clustered according to protein sequence. Lignin content in tuberous root increased during PPD, and 27 *MeCAD* genes may play a crucial role in PPD. Among them, *MeCAD13* and *MeCAD28* enhanced wound stress tolerance of transgenic yeast cells. Moreover, silencing *MeCAD13* and *MeCAD28* significantly decreased the lignin content in cassava leaves. Overall, the results provide new insight for cassava engineering programs, including improve PPD tolerance and increase lignin content.

Supplementary Materials: The following supporting information can be downloaded at the website of this paper posted on Preprints.org.

Authorship Contribution Conceptualization, original draft preparation, F. A.; software, review and editing, visualization, T. C.; methodology and project administration, W. Z.; data analysis, H. X.; validation form analysis, J. X.; data curation, X. L.; investigation, Z.W.; resources, K.L.; supervision, S.C. and J.C. All authors have read and agreed to the published version of the manuscript.

Funding: This work was financially supported by Natural Science Foundation of China (NSFC) Projects (No. 32460521), Project of National Key Laboratory for Tropical Crop Breeding (No. NKLTCB202334), National Key Research and Development Program of China (No. 2023YFD1200204), and Chinese Academy of Tropical Agricultural Sciences for Science and Technology Innovation Team (NO. CATASCXTD202301). We acknowledge Wentao Shen, Pu Yan and Decai Tuo for their technical assistance.

Data Availability The complete data sets generated in our study have been submitted in the NCBI Sequence Read Archive database (BioProject PRJNA1143580).

Conflicts of Interest We declare that we do not have any commercial or associative interest that represents a conflict of interest in connection with the work submitted.

References

1. Mohidin: S. R. N. S. P., Moshawih, S., Hermansyah, A., Asmuni, M. I., Shafqat, N., Ming, L. C. Cassava (*Manihot esculenta* Crantz): A systematic review for the pharmacological activities, traditional uses, nutritional values, and phytochemistry. J. Evid. Based Integr. Med. **2023,** *28,* 2515690X231206227.
2. FAOSTAT. FAOSTAT statistical database, agriculture data. **2022,** http://apps.fao.org.
3. Lebot, V., Lawac, F., Muñoz-Cuervo, I., Mercier, P. E., Legendre, L. Metabolite fingerprinting of cassava (*Manihot esculenta* Crantz) landraces assessed for post-harvest physiological deterioration (PPD). Food Chem. **2023**, *421,* 136217.
4. Li, R., Yuan, S., Zhou, Y., Wang, S., Zhou, Q., Ding, Z., Wang, Y., Yao, Y., Liu, J., Guo, J. Comparative transcriptome profiling of cassava tuberous roots in response to postharvest physiological deterioration. Int. J. Mol. Sci. **2023**, *24,* 246.
5. Zainuddin, I. M., Fathoni, A., Sudarmonowati, E., Beeching, J. R., Gruissem, W., Vanderschuren, H. Cassava post–harvest physiological deterioration: From triggers to symptoms. Postharvest Biol. Technol. **2018,** *142,* 115-123.
6. An, F., Xue, J., Luo, X., Chen, T., Wei, Z., Zhu, W., Ou, W., Li, K., Cai, J., Chen, S. MePOD12 participates the regulation to postharvest physiological deterioration by ROS scavenging and lignin accumulation in cassava tuberous roots. Postharvest Biol. Technol. **2024**, *207,* 112609.
7. Wahengbam, E. D., Devi, C. P., Sharma, S. K., Roy, S. S., Maibam, A., Dasgupta, M., Luikham, S., Chongtham, T., Ningombam, A., Bhupenchandra, I., Singh, L. K., Devi, Y. P., Thokchom, S., Khaba, C. I., Singh, N. B., Rajashekar, Y., Das, S., Mohanty, S., Sahoo, M. R. Reactive oxygen species turnover, phenolics metabolism, and some key gene expressions modulate postharvest physiological deterioration in cassava tubers. Front. Microbiol. **2023,** *14,* 1148464.

 doi:10.20944/preprints202409.2434.v1

8. Djabou, A. S. M., Carvalho, L. J. C. B., Li, Q., Niemenak, N., Chen, S. Cassava postharvest physiological deterioration: a complex phenomenon involving calcium signaling, reactive oxygen species and programmed cell death. Acta. Physiol. Plant. **2017,** *39,* 91.
9. Zidenga, T., Leyva-Guerrero, E., Moon, H., Siritunga, D., Sayre, R. Extending cassava root shelf life via reduction of reactive oxygen species production. Plant Physiol. **2012,** *159,* 1396-1407.
10. Xu, J., Duan, X., Yang, J., Beeching, J. R., Zhang, P. Enhanced reactive oxygen species scavenging by overproduction of superoxide dismutase and catalase delays postharvest physiological deterioration of cassava storage roots. Plant Physiol. **2013,** *161,* 1517-1528.
11. Oirschot, Q. E. A. v., Rees, D., Aked, J., Kihurani, A. Sweetpotato cultivars differ in efficiency of wound healing. Postharvest Biol. Technol. **2006,** *42,* 65-74.
12. Wang, B., Jiang, H., Bi, Y., He, X., Wang, Y., Li, Y., Zheng, X., Prusky, D. Preharvest multiple sprays with sodium nitroprusside promote wound healing of harvested muskmelons by activation of phenylpropanoid metabolism. Postharvest Biol. Technol. **2019,** *158,* 110988.
13. Zhao, Y., Deng, L., Zhou, Y., Ming, J., Yao, S., Zeng, K. Wound healing in citrus fruit is promoted by chitosan and Pichia membranaefaciens as a resistance mechanism against Colletotrichum gloeosporioides. Postharvest Biol. Technol. **2018,** *145,* 134-143.
14. Reilly, K., G´omez-V´asquez, R., Buschmann, H., Tohme, J., Beeching, J. R. Oxidative stress responses during cassava post-harvest physiological deterioration. Plant Mol. Biol. **2003,** *53,* 669-685.
15. Weng, J. and Chapple, C. The origin and evolution of lignin biosynthesis. New Phytol. **2010,** *187,* 273-285.
16. Ge, X., Zhu, Y., Li, Z., Bi, Y., Yang, J., Zhang, J., Prusky, D. Preharvest multiple fungicide stroby sprays promote wound healing of harvested potato tubers by activating phenylpropanoid metabolism. Postharvest Biol. Technol. **2021,** *171,* 111328.
17. Kim, Y. H., Bae, J. M., Huh, G. H. Transcriptional regulation of the cinnamyl alcohol dehydrogenase gene from sweetpotato in response to plant developmental stage and environmental stress. Plant Cell Rep **2010,** *29,* 779-791.
18. Goujon, T., Sibout, R., Eudes, A., MacKay, J., Jouanin, L. Genes involved in the biosynthesis of lignin precursors in Arabidopsis thaliana. Plant Physiol. Biochem. **2003,** *41,* 677-687.
19. Zhu, Y., Wang, Y., Jiang, H., Liu, W., Zhang, S., Hou, X., Zhang, S., Wang, N., Zhang, R., Chen, X. Transcriptome analysis reveals that PbMYB61 and PbMYB308 are involved in the regulation of lignin biosynthesis in pear fruit stone cells. Plant J. **2023,** *116,* 217-233.
20. Dong, N. Q. and Lin, H. X. Contribution of phenylpropanoid metabolism to plant development and plant-environment interactions. J. Integr. Plant Biol. **2021,** *63,* 180-209.
21. Yan, Y., Wang, P., Lu, Y., Bai, Y., Wei, Y., Liu, G., Shi, H. MeRAV5 promotes drought stress resistance in cassava by modulating hydrogen peroxide and lignin accumulation. Plant J. **2021,** *107,* 847-860.
22. Liu, Q., Luo, L., Zheng, L. Lignins: biosynthesis and biological functions in plants. Int. J. Mol. Sci. **2018,** *19,* 335.
23. Kim, S., Kim, M., Bedgar, D. L., Moinuddin, S. G. A., Cardenas, C. L. Functional reclassification of the putative cinnamyl alcohol dehydrogenase multigene family in *Arabidopsis*. PNAS **2004,** *101,* 1455-1460.
24. Liu, X., Acker, R. V., Voorend, W., Pallidis, A., Goeminne, G., Pollier, J., Morreel, K., Kim, H., Muylle, H., Bosio, M., Ralph, J., Vanholme, R., Boerjan, W. Rewired phenolic metabolism and improved saccharification efficiency of a Zea mays cinnamyl alcohol dehydrogenase 2 (zmcad2) mutant. Plant J. **2021,** *105,* 1240-1257.
25. Ibrahim, W., Zhu, Y. M., Chen, Y., Qiu, C. W., Zhu, S., Wu, F. Genotypic differences in leaf secondary metabolism, plant hormones and yield under alone and combined stress of drought and salinity in cotton genotypes. Physiol. Plantarum **2019,** *165,* 343-355.
26. Jiao, F., Luo, R., Dai, X., Liu, H., Yu, G., Han, S., Lu, X., Su, C., Chen, Q., Song, Q., Liu, W., Jiang, Y., Jin, Y., Wang, C., Yang, J., Qi, H. Drought-induced ABA, H_2O_2 and JA positively regulate *CmCAD* genes and lignin synthesis in melon stems. BMC Plant Biol. **2021,** *21,* 83.
27. Tobias, C. M. and Chow, E. K. Structure of the cinnamyl-alcohol dehydrogenase gene family in rice and promoter activity of a member associated with lignification. Planta **2005,** *220,* 678-688.
28. Barakat, A., Bagniewska-Zadworna, A., Choi, A., Plakkat, U., DiLoreto, D., Yellanki, P., Carlson, J. E. The cinnamyl alcohol dehydrogenase gene family in Populus: phylogeny, organization, and expression. BMC Plant Biol. **2009,** *9,* 26.
29. Chao, N., Huang, S., Kang, X., Yidilisi, K., Dai, M., Liu, L. Systematic functional characterization of cinnamyl alcohol dehydrogenase family members revealed their functional divergence in lignin biosynthesis and stress responses in mulberry. Plant Physiol. Bioch. **2022**, *186,* 145-156.
30. Qi, K., Song, X., Yuan, Y., Bao, J., Gong, X., Huang, X., Khanizadeh, S., Zhang, S., Tao, S. CAD genes: genome-wide identification, evolution, and their contribution to lignin biosynthesis in Pear (*Pyrus bretschneideri*). Plants **2021,** *10,* 1444.

31. Sibout, R., Eudes, A., Mouille, G., Pollet, B., Lapierre, C., Jouanin, L., Séguin, A. CINNAMYL ALCOHOL DEHYDROGENASE-C and -D are the primary genes involved in lignin biosynthesis in the floral stem of *Arabidopsis*. Plant Cell **2005,** *17,* 2059-2076.
32. Jin, Y., Zhang, C., Liu, W., Qi, H., Chen, H., Cao, S. The cinnamyl alcohol dehydrogenase gene family in Melon (*Cucumis melo* L.): bioinformatic analysis and expression patterns. PLOS ONE **2014,** *9,* e101730.
33. Cheng, H., Li, L., Xu, F., Cheng, S., Cao, F., Wang, Y., Yuan, H., Jiang, D., Wu, C. Expression patterns of a cinnamyl alcohol dehydrogenase gene involved in lignin biosynthesis and environmental stress in *Ginkgo biloba*. Mol. Biol. Rep. **2013,** *40,* 707-721.
34. Ma, Q. Functional analysis of a cinnamyl alcohol dehydrogenase involved in lignin biosynthesis in wheat. J. Exp. Bot. **2010,** *10,* 2735-2744.
35. Saballos, A., Ejeta, G., Sanchez, E., Kang, C., Vermerris, W. A genomewide analysis of the cinnamyl alcohol dehydrogenase family in sorghum [*Sorghum bicolor* (L.) Moench] identifies *SbCAD2* as the *Brown midrib6* gene. Genetics **2009,** *181,* 783-795.
36. Deng, W., Zhang, M., Wu, J., Jiang, Z., Tang, L., Li, Y., Wei, C., Jiang, C., Wan, X. Molecular cloning, functional analysis of three cinnamyl alcohol dehydrogenase (CAD) genes in the leaves of tea plant, Camellia sinensis. J. Plant Physiol. **2013,** *170,* 272-282.
37. Zhang, K., Qian, Q., Huang, Z., Wang, Y., Li, M., Hong. L., Zeng, D., Gu, M., Chu, C., Cheng, Z. Gold Hull and internode2 encodes a primarily multifunctional cinnamyl-alcohol dehydrogenase in rice. Plant Physiol. **2006,** *140,* 972-983.
38. Bukh, C., Nord-Larsen, P. H., Rasmussen, S. K. Phylogeny and structure of the cinnamyl alcohol dehydrogenase gene family in *Brachypodium distachyon*. J. Exp. Bot. **2012,** *63,* 6223-6236.
39. Tronchet, M., Balague, C., Kroj, T., Jouanin, L., Roby, D. Cinnamyl alcohol dehydrogenases-C and D, key enzymes in lignin biosynthesis, play an essential role in disease resistance in Arabidopsis. Mol. Plant Pathol. **2010,** *11,* 83-92.
40. An, F., Xiao, X., Chen, T., Xue, J., Luo, X., Ou, W., Li, K., Cai, J., Chen, S. Systematic analysis of bHLH transcription factors in cassava uncovers their roles in postharvest physiological deterioration and cyanogenic glycosides biosynthesis. Front. Plant Sci. **2022,** *13,* 901128.
41. Bano, N., Patel, P., Chakrabarty, D., Bag, S. K. Genome-wide identification, phylogeny, and expression analysis of the bHLH gene family in tobacco (*Nicotiana tabacum*). Physiol. Mol. Biol. Plants **2021,** *27,* 1747-1764.
42. Moura, J. C. M. S., Bonine, C. A. V., Viana, J. O. F., Dornelas, M. C., Mazzafera, P. Abiotic and biotic stresses and changes in lignin content and composition in plants. J. Integ. Plant Biol. **2010,** *52,* 360-376.
43. Hamann, T. Plant cell wall integrity maintenance as an essential component of biotic stress response mechanisms. Front. Plant Sci. **2012,** *3,* 77.
44. Naoumkina, M. A., Zhao, Q., Gallego-Giraldo, L., Dai, X., Zhao, P. X., Dixon, R. A. Genome-wide analysis of phenylpropanoid defense pathways. Mol. Plant Pathol. **2010,** *11,* 829-846.
45. Wang, C., Wu, J., Tang, Y., Min, Y., Wang, D., Ma, X., Li, H., Li, J., Chen, Y., Chen, S., Liu, Z. Understanding the changes of phenylpropanoid metabolism and lignin accumulation in wounded cassava root during postharvest storage. Sci. Hortic. **2023,** *310,* 111765.
46. Li Z, Xue, S., Xu, X., Wang, B., Zheng, X., Li, B., Xie, P., Bi, Y., Prusky, D. Preharvest multiple sprays with chitosan accelerate the deposition of suberin polyphenolic at wound sites of harvested muskmelons. Postharvest Biol. Tec. **2021,** *179,* 111565.
47. Rahmawati, R., Khumaida, N., Ardie, S., Sukma, D., Sudarsono. Effects of harvest period, storage, and genotype on postharvest physiological deterioration response in cassava. Biodiversitas **2022,** *23,* 100-109.
48. Yan, P., Zeng, Y., Shen, W., Tuo, D., Li, X., Zhou, P. Nimble cloning: A simple, versatile, and efficient system for standardized molecular cloning. Front. Bioeng. Biotech. **2020,** *7,* 460.
49. Tuo, D., Zhou, P., Yan, P., Cui, H., Liu, Y., Wang, H., Yang, X., Liao, W., Sun, D., Li, X., Shen, W. A cassava common mosaic virus vector for virus-induced gene silencing in cassava. Plant Methods **2021,** *17,* 74.
50. Foster, C., Martin, T., Pauly, M. Comprehensive compositional analysis of plant cell wall (Lignocellulosic biomass) Part II: carbohydrates. J. Vis. Exp. **2010,** *37,* e1837.